Optics Letters

Reduction of absorption losses in MOVPE-grown AlGaAs Bragg mirrors

JOHANNES POHL,[1] GARRETT D. COLE,[2,3] UTE ZEIMER,[1] MARKUS ASPELMEYER,[2] AND MARKUS WEYERS[1,*]

[1]Ferdinand-Braun-Institut, Leibniz-Institut für Höchstfrequenztechnik (FBH), 12489 Berlin, Germany
[2]Vienna Center for Quantum Science and Technology (VCQ), Faculty of Physics, University of Vienna, 1090 Vienna, Austria
[3]Crystalline Mirror Solutions LLC and GmbH, Santa Barbara, California 93101, USA and 1060 Vienna, Austria
*Corresponding author: markus.weyers@fbh-berlin.de

Received 8 May 2018; revised 14 June 2018; accepted 17 June 2018; posted 18 June 2018 (Doc. ID 330996); published 19 July 2018

Residual *p*-type doping from carbon has been identified as the root cause of excess absorption losses in (Al)GaAs/AlGaAs Bragg mirrors for high-finesse optical cavities when grown by metalorganic vapor phase epitaxy (MOVPE). Through optimization of the growth parameters with the aim of realizing low carbon uptake, we have shown a path for decreasing the parasitic background absorption in these mirrors from 100 to the 10 ppm range near 1064 nm. This significant reduction is realized via compensation of the carbon acceptors by intentional doping with the donor silicon in the uppermost layer pairs of 40-period GaAs/AlGaAs Bragg mirrors. Thus, we find that such compensation enables MOVPE-derived multilayer mirrors with the potential for a high cavity finesse (>100,000 in the near infrared) approaching the performance levels found with Bragg mirrors grown by molecular beam epitaxy (MBE).

Published by The Optical Society under the terms of the Creative Commons Attribution 4.0 License. Further distribution of this work must maintain attribution to the author(s) and the published article's title, journal citation, and DOI.

OCIS codes: (160.6000) Semiconductor materials; (230.1480) Bragg reflectors; (230.4040) Mirrors; (230.4170) Multilayers; (230.5750) Resonators; (310.6860) Thin films, optical properties.

https://doi.org/10.1364/OL.43.003522

Crystalline Al(Ga)As/Al(Ga)As distributed Bragg reflectors (DBRs) are core building blocks for optoelectronic devices such as light emitting diodes (LEDs) and vertical-cavity surface-emitting lasers (VCSELs) from the red wavelength range near 650 nm [1] to the NIR spectral region, as well as optically pumped photonic structures including semiconductor disk lasers (SCDLs) [2] and semiconductor saturable absorber mirrors (SESAMs) [3]. Moreover, arsenide DBRs find increasing interest in a wide range of application areas, including precision metrology [4], high-power lasers [5], and mid-IR spectroscopy [6]. This is because crystalline semiconductor coatings exhibit superior physical properties when compared to typical SiO_2/Ta_2O_5-based dielectric reflectors deposited via ion-beam sputtering (IBS). Specifically, these single-crystal Bragg reflectors exhibit an order of magnitude improvements with respect to Brownian noise, thermal conductivity, and absorption in the mid-IR spectral region [7]. These advantageous properties were initially explored through the development of free-standing mirrors for cavity optomechanic experiments as realized via selective wet chemical or gas-phase etching [8,9]. Our earlier work showed that the optical quality of DBRs grown by metalorganic vapor phase epitaxy (MOVPE) was lower than expected when compared with the simulated maximum reflectivity values. To further improve the performance of high-reflectivity GaAs/AlGaAs Bragg mirrors for use as suspended optomechanical resonators or as end mirrors for stabilizing laser cavities, the root cause for the higher than expected optical losses needed to be found. To this end, we pursued an in-depth analysis of the as-grown layer stacks with a key measurement technique being photothermal common path interferometry (PCI) [10]. Additionally, we investigated modifications to the standard MOVPE growth process including varying the substrate miscut, composition of the individual mirror layers, and growth temperature. Finally, we introduced intentional doping with Si to compensate the residual carbon acceptors found in the structure. This latter effort turned out to be the most effective approach for bringing the absorption in the mirror stack down to the 10 ppm range.

Al(Ga)As/(Al)GaAs DBRs consisting of alternating $\lambda/4$ layers (for a target wavelength of 1064 nm) with low Al content (high refractive index) and high Al content (low refractive index) were grown on 2-in.-diameter laser-grade *n*-type GaAs substrates of high crystalline quality (etch pit density below 100 cm^{-2}) with exact orientation. Growth by MOVPE was performed in an AIX 200/4 horizontal reactor in a 3×2 in. configuration using the standard precursors arsine, trimethylgallium, and trimethylaluminum. For *n*-type doping in our compensation experiments, disilane diluted in hydrogen was used. Because most of the light within the DBR stop band is reflected by the uppermost mirror layers (with a typical energy penetration depth on the order of 200 nm or less for light

incident from vacuum or air [11]), the total number of mirror periods can be varied without altering the impact of loss processes beyond the mirror transmission. Thus, three identical base mirrors with 36 or 40 layer pairs were grown as templates. Onto these templates an additional 6–10 layer pairs were grown under various growth conditions to explore their impact on the maximum DBR reflectivity. This not only helped to reduce the overall time for a series of experiments, but also allowed for the deposition of the uppermost layers in parallel onto semi-insulating substrates, thereby making their electrical properties accessible. The starting point for the study towards ultralow-loss MOVPE-grown DBRs was a 40-period $Al_{0.12}Ga_{0.88}As/Al_{0.92}Ga_{0.08}As$ mirror as described in Ref. [12]. Figure 1(a) shows the X-ray rocking curve of this mirror with well-resolved superlattice peaks. The fitted curve reveals that the targeted compositions and thicknesses have been realized with good accuracy. The Bragg mirrors are characterized for their reflectance spectrum via spectrophotometry as shown in Fig. 1(b).

Using the values obtained from fitting the X-ray rocking curve for the simulation of the reflectivity spectrum yields very good agreement with the measured spectrum, not only with respect to the stop band but also the sideband oscillations. Using a transfer matrix approach, the simulated reflectivity for this structure is 99.995%. Precise measurements of this value as described in the next section, however, reveal a lower reflectivity of somewhat above 99.98% associated with absorption losses in the 60–80 ppm range. This level of absorption is incompatible with a cavity finesse value of $>10^5$ which would require total per mirror losses of ≤ 30 ppm.

The electrical properties of test structures grown on semi-insulating substrates were assessed by contactless sheet resistivity

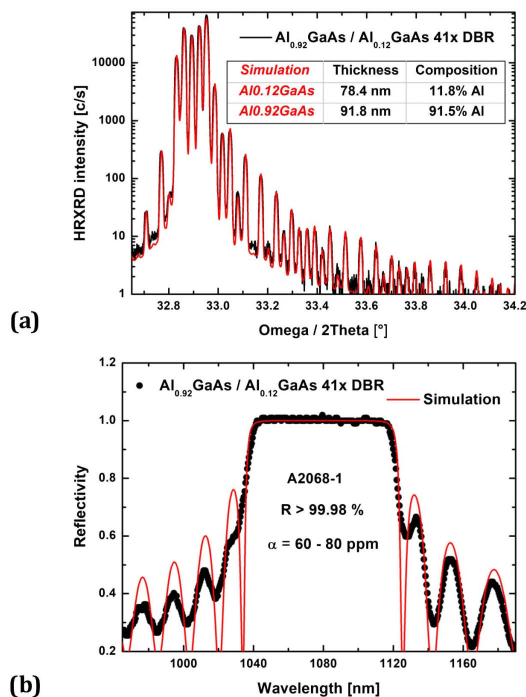

Fig. 1. X-ray diffraction and reflectance analysis of the baseline mirror structure. (a) HRXRD measurement and simulation of an $Al_{0.92}Ga_{0.08}As/Al_{0.12}Ga_{0.88}As$ DBR with 41 layer pairs; (b) measured reflectivity spectrum compared to simulated spectrum [based on HRXRD results shown in (a)].

measurements based on the damping of Eddy currents. These relatively quick and simple nondestructive measurements were cross-checked against Hall effect measurements that require cleaving of 10 mm × 10 mm samples and formation of ohmic contacts at the corners. Both methods yield the same sheet resistivity values. The carbon concentration was measured by calibrated secondary ion mass spectrometry (SIMS). Due to the high affinity of Al to oxygen, AlGaAs is known to be prone to oxygen incorporation, especially at high Al content. However, SIMS showed low oxygen content only slightly above the detection limit of $1–2 \times 10^{15}$ cm^{-3}. Thus, oxygen does not appear to play a relevant role in these layers and is not discussed further.

The absolute reflectivity of the mirrors is characterized via optical ringdown, in this case by forming a linear cavity using a curved IBS-coated dielectric mirror as the input coupler and the mirror under test as the back reflector. Measuring the decaying optical intensity of the cavity on a photodiode upon switching off a laser signal injected on resonance, we can extract the finesse, F, from the cavity length, L, and recorded decay rate, τ ($F = \pi c\tau/L$). From the finesse, the absolute reflectivity of the mirrors can be determined via $F = \pi\sqrt{R1R2}/(1 - \sqrt{R1R2})$, where R1 and R2 are the reflectance of the cavity end mirrors. We calibrate the reflectivity of the IBS input coupler by first forming a cavity from two nominally identical mirrors (from the same sputtering run) and measuring their finesse and thus reflectance. This known mirror is then used as the input coupler in further experiments with the GaAs-based DBRs. The total optical losses of the mirrors under test is ultimately $T + S + A$, with the reflectance $R = 1 - (T + S + A)$, and with the three loss components being the mirror transmission T (controlled by the refractive index contrast and number of periods in the DBR), scatter S (controlled by the mirror microroughness and surface defect density), and finally absorption A (which to the best of our knowledge (and as demonstrated by our results) in these semiconductor heterostructures is controlled by the background doping and thermally excited free carriers).

The mirror transmission can be modeled using the known layer structure, refractive indices, and as-grown layer thicknesses (extracted via X-ray and spectrophotometry measurements as described above). This then leaves scatter and absorption as unknowns. We independently extract the mirror absorption via direct PCI measurements [10]. In this technique, a chopped Watt-level pump laser (operating here at 1064 nm) is used to generate a time-modulated thermal lens on the sample surface, the magnitude of which is read out using a weak off-axis probe beam. Given the rapid thermal transport through the Bragg mirror, the thermal deflection is dominated by the substrate. Through careful calibration of the substrate response, the mirror absorption can be directly extracted. Finally, with calculations of the DBR penetration depth [11], the material absorption coefficient can be determined. With the transmission and absorption known, the only remaining loss component is then scatter, which can be determined via simple arithmetic.

The baseline mirrors were designed for the wet-chemical etching processes for the fabrication of optomechanical resonators [12] with $Al_{0.92}Ga_{0.08}As$ as low index layers to avoid the rapid oxidation of AlAs under ambient conditions, and $Al_{0.12}Ga_{0.88}As$ as the high index layers to enable selective etching of the underlying GaAs substrate for manufacturing suspended micromirrors. The high Al-content AlGaAs layers are known to be prone to uptake of carbon which is a shallow

acceptor in AlGaAs [13]. Thus, free-carrier absorption due to the p-type background doping was suspected to be the reason for the lower than expected reflectivity and the higher than desired absorption loss. Figure 2(a) shows that the carbon uptake in $Al_{0.92}Ga_{0.08}As$ is approximately 4×10^{17} cm^{-3} at the standard growth temperature of 770°C and drops to about 1×10^{17} cm^{-3} at 650°C. However, reduction of the growth temperature is not a viable route for layers with such high Al content because of the potential for excess roughness due to the reduced Al mobility, which will also yield reduced reflectivity from optical scatter [14].

The tendency for roughening is reduced when the Al content is reduced. Additionally, the C uptake is also reduced. When growing at 770°C, the C content in $Al_{0.5}Ga_{0.5}As$ is approximately one order of magnitude lower than in $Al_{0.92}Ga_{0.08}As$. A decreased growth temperature yields a further reduction in C uptake, although less pronounced than for the high Al content. Figure 2(b) shows that even for this medium-Al content the surface gets rougher when going to low growth temperature. To balance these competing issues, a hybrid approach was taken. Because the reduction of the Al content in the low index layers also reduces the index contrast and thus the reflectivity, we grew six additional $Al_{0.5}Ga_{0.5}As/Al_{0.12}Ga_{0.88}As$ layer pairs on top of two of the baseline mirror stacks of Fig. 1 at the original high temperature of 770°C and at the reduced temperature of 650°C.

However, this approach did not yield the desired result. Despite the lower C uptake in the upper layer pairs, the absorption remained high (near 100 ppm) for the high growth temperature (while yielding the smoother morphology) and was only slightly reduced at the lower growth temperature. The main driver for the excess optical absorption was the

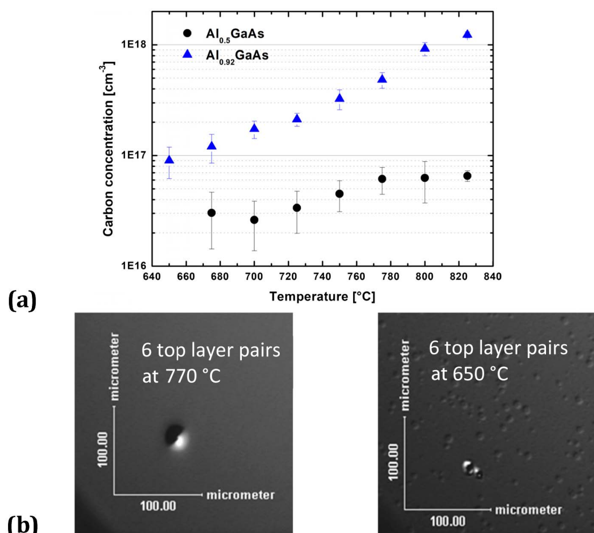

Fig. 2. Carbon uptake in MOVPE-grown ternary AlGaAs alloys as a function of growth temperature, as well as an overview of the as-grown mirror surface quality. (a) Carbon concentration from SIMS versus growth temperature for high ($x = 0.92$) and medium ($x = 0.5$) Al content. (b) Optical microscopy images of two mirrors with identical 40-fold bottom layer pairs $Al_{0.92}Ga_{0.08}As/Al_{0.12}Ga_{0.88}As$ and additional six top layer pairs of $Al_{0.5}Ga_{0.5}As/Al_{0.12}Ga_{0.88}As$ grown at 770°C (left) and 650°C (right) together with measured absorption.

increased optical penetration depth in the mirror, so although the individual absorption coefficients of the mirror materials were reduced to 1.3 cm^{-1} in the DBR with the low index $Al_{0.5}Ga_{0.5}As$ layers versus ~2 cm^{-1} in the baseline structure, the increased energy penetration depth (345 nm for the $Al_{0.12}Ga_{0.88}As/Al_{0.5}Ga_{0.5}$ surface layers compared with 192 nm for the baseline $Al_{0.12}Ga_{0.88}As/Al_{0.92}Ga_{0.08}As$ structures) led to a larger overall absorption loss value of approximately 90 ppm. From this result, it is clear that the key to improved performance will be to both reduce the background doping in the mirror while simultaneously minimizing the field penetration (by enhancing the refractive index contrast of the constituent mirror materials).

For large-area substrate-transferred mirrors, as opposed to suspended micromirrors, the need for Al incorporation into the high index layers is no longer valid because the selective etching procedure is unnecessary for the fabrication of such bulk optics. Going from $Al_{0.12}Ga_{0.88}As$ to GaAs additionally yields a slightly higher index contrast, further reducing the energy penetration depth at 1064 to 163 nm. The index contrast could further be increased by using AlAs for the low index layers. However, this makes the layer stacks sensitive to lateral oxidation when the wafer is cleaved into chips or etched into small resonators. Here, the addition of Ga is known to significantly improve the material stability [15] and thus $Al_{0.92}Ga_{0.08}As$ was used for the low index layers as a compromise for a reduced oxidation rate with acceptable index contrast. The shorter penetration depth in these mirrors reduced the absorption to about 40 ppm for a 46-period stack grown at 770°C [see asterisk in Fig. 3(b)]. When growing the stack at 720°C, this value was further reduced to 18 ppm. The smaller absorption at the lower growth temperature again can be attributed to the lower C background doping. Still, these values are not in the single digit or even subppm range as required for high-finesse ($>10^5$) reference cavities [16].

To test the assumption that free carrier absorption is the root cause of the excess absorption in our MOVPE-grown DBRs, base mirrors with 36 layer pairs were grown at 770°C. These were then overgrown with 10 layer pairs that were intentionally doped with Si at 770°C and 720°C. Additionally, a semi-insulating substrate was overgrown with the final 10 layer pairs in the same growth run. Figure 3 summarizes the results of the electrical characteristics together with the measured absorption values via PCI at 1064 nm against the disilane flow rate injected into the reactor. For the initially used high growth temperature of 770°C, the electrical characterization was done by contactless sheet resistivity measurements (squares) and by Hall effect measurements (dots). Both methods yield nearly identical results [Fig. 3(a)]. Without the addition of disilane, a sheet resistivity of approximately 800 Ωcm^{-2} is obtained [see asterisk in Fig. 3(b)]. The resistivity increases up to about 3300 Ωcm^{-2} for 0.16 sccm of disilane and then drops again to approximately 2500 Ωcm^{-2} when the layer turns n-type. With increasing sheet resistivity, the absorption drops from 40 ppm to slightly below 20 ppm where it stays also when the p-doping is slightly overcompensated and the layer turns n-type. This is in line with the lower free-carrier losses observed in n-type AlGaAs-based VCSEL mirrors as compared to p-type ones [17]. However, while this is generally accepted and a factor of about three higher absorption for p-type compared to n-type at higher doping levels has been reported [18], no reliable literature values on

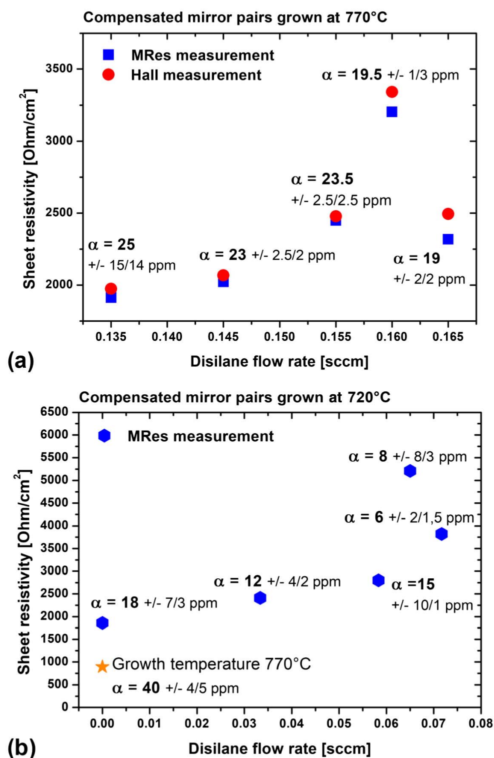

Fig. 3. Sheet resistivity of 10 $Al_{0.92}Ga_{0.08}As$/GaAs layer pairs (on semi-insulating substrate) versus flow rate of the dopant source disilane (a) grown at 770°C and (b) grown at 720°C. The absorption values of these 10 layers grown in parallel on base mirrors without compensation by Si doping (36 pairs) are given at each data point. The asterisk in (b) marks the value for a stack grown at 770°C without Si doping.

free-carrier absorption at low background doping in AlGaAs layers could be found.

For the lower growth temperature of 720°C, the undoped 10 layer stack shows more than double the sheet resistivity (approximately 1800 Ωcm^{-2}) than that grown at high temperature [Fig. 3(b)]. Additionally, compensation is achieved at less than half the disilane flow (about 0.07 sccm) and yields a higher sheet resistance of more than 5000 Ωcm^{-2}. These findings are in line with the lower carbon background at lower temperature. This then finally allowed a reduction of the absorption to the single digit region with 8 ppm for the highest sheet resistivity multilayer. Going slightly to the *n*-side, the low absorption is maintained. This result is a significant improvement over our baseline absorption values as well as those for nonoptimized structures which were typically in the 40–50 ppm range.

In conclusion, free-carrier absorption due to *p*-type background doping with carbon has been identified as an important absorption mechanism in low-loss AlGaAs Bragg mirrors grown by MOVPE. Minimizing carbon incorporation through the use of a reduced growth temperature of 720°C resulted in a reduction of absorption losses from 40–50 ppm to about 20 ppm. Compensating the acceptor carbon by doping with the donor Si allowed for a further reduction into the single-digit ppm range. This qualifies MOVPE material for applications requiring a modestly low absorption value (on the order of 10 ppm). The reduction achieved by compensation doping now allows one to also leverage the capability of MOVPE for strain compensation by adding *P* to the layer stack [19]. This gives an additional degree of freedom in the design of crystalline Bragg mirrors for low-loss cavities. The low absorption values below 1 ppm obtained with $GaAs/Al_{0.92}Ga_{0.08}As$ mirrors grown by molecular beam epitaxy (MBE) [16,7] remain a challenging but interesting future target for MOVPE.

Funding. Deutsche Forschungsgemeinschaft (DFG) (WE1908/6-1); Austrian Science Fund (FWF) (I909/N16, L426, START); Directorate-General for Research and Innovation (IQOS, Marie Curie Fellowship GDC, MINOS).

Acknowledgment. Microfabrication was carried out at the Zentrum für Mikro- und Nanostrukturen (ZMNS) of the Technische Universität Wien. The authors also thank Alexei Alexandrovski of Stanford Photothermal Solutions (SPTS) for his assistance with direct absorption measurements via PCI.

REFERENCES

1. A. Knigge, M. Zorn, M. Weyers, and G. Tränkle, Electron. Lett. **38**, 882 (2002).
2. F. Saas, V. Talalaev, U. Griebner, J. W. Tomm, M. Zorn, and M. Weyers, Appl. Phys. Lett. **89**, 151120 (2006).
3. M. Zorn, P. Klopp, F. Saas, A. Ginolas, O. Krüger, U. Griebner, and M. Weyers, J. Cryst. Growth **310**, 5187 (2008).
4. G. D. Cole, W. Zhang, M. J. Martin, J. Ye, and M. Aspelmeyer, Nat. Photonics **7**, 644 (2013).
5. A. Diebold, T. Zengerle, C. G. E. Alfieri, C. Schriber, F. Emaury, M. Mangold, M. Hoffmann, C. J. Saraceno, M. Golling, D. Follman, G. D. Cole, M. Aspelmeyer, T. Südmeyer, and U. Keller, Opt. Express **24**, 10512 (2016).
6. B. J. Bjork, T. Q. Bui, O. H. Heckl, P. B. Changala, B. Spaun, P. Heu, D. Follman, C. Deutsch, G. D. Cole, M. Aspelmeyer, M. Okumura, and J. Ye, Science **354**, 444 (2016).
7. M. Marchiò, R. Flaminio, L. Pinard, D. Forest, C. Deutsch, P. Heu, D. Follman, and G. D. Cole, Opt. Express **26**, 611 (2018).
8. G. D. Cole, S. Gröblacher, K. Gugler, S. Gigan, and M. Aspelmeyer, Appl. Phys. Lett. **92**, 261108 (2008).
9. G. D. Cole, Y. Bai, M. Aspelmeyer, and E. A. Fitzgerald, Appl. Phys. Lett. **96**, 261102 (2010).
10. A. Alexandrovski, M. Fejer, A. Markosian, and R. Route, Proc. SPIE **7193**, 7193D (2009).
11. D. I. Babic and S. W. Corzine, IEEE J. Quantum Electron. **28**, 514 (1992).
12. G. D. Cole, I. Wilson-Rae, M. R. Vanner, S. Gröblacher, J. Pohl, M. Zorn, M. Weyers, A. Peters, and M. Aspelmeyer, *IEEE 23rd International Conference on Micro Electro Mechanical Systems (MEMS)* (2010), p. 5442339.
13. T. F. Kuech, M. A. Tischler, R. Potemski, F. Cardone, and G. Scilla, J. Cryst. Growth **98**, 174 (1989).
14. A. Bhattacharya, M. Nasarek, U. Zeimer, A. Klein, M. Zorn, F. Bugge, S. Gramlich, and M. Weyers, J. Cryst. Growth **274**, 331 (2005).
15. F. Reinhardt, B. Dwir, and E. Kapon, Appl. Phys. Lett. **68**, 3168 (1996).
16. G. D. Cole, W. Zhang, B. J. Bjork, D. Follman, P. Heu, C. Deutsch, L. Sonderhouse, J. Robinson, C. Franz, A. Alexandrovski, M. Notcutt, O. H. Heckl, J. Ye, and M. Aspelmeyer, Optica **3**, 647 (2016).
17. D. I. Babic, J. Piprek, K. Streubel, R. P. Mirin, N. M. Margalit, D. E. Mars, J. E. Bowers, and E. L. Hu, IEEE J. Quantum Electron. **33**, 1369 (1997).
18. H. C. Casey, D. D. Sell, and K. W. Wecht, J. Appl. Phys. **46**, 205 (1975).
19. A. Maaßdorf and M. Weyers, J. Cryst. Growth **414**, 10 (2015).